

Evolution of the proton sd states in neutron-rich Ca isotopes

M. Grasso,^{1,2} Z.Y. Ma,^{3,4} E. Khan,¹ J. Margueron,¹ and N. Van Giai¹

¹*Institut de Physique Nucléaire, Université Paris-Sud, IN2P3-CNRS, F-91406 Orsay Cedex, France*

²*Dipartimento di Fisica e Astronomia and INFN, Via Santa Sofia 64, I-95123 Catania, Italy*

³*China Center of Advanced Science and Technology (World Laboratory), Beijing 100080, China*

⁴*China Institute of Atomic Energy, Beijing 102413, China*

We analyze the evolution with increasing isospin asymmetry of the proton single-particle states $2s1/2$ and $1d3/2$ in Ca isotopes, using non-relativistic and relativistic mean field approaches. Both models give similar trends and it is shown that this evolution is sensitive to the neutron shell structure, the two states becoming more or less close depending on the neutron orbitals which are filled. In the regions where the states get closer some parametrizations predict an inversion between them. This inversion occurs near ^{48}Ca as well as very far from stability where the two states systematically cross each other if the drip line predicted in the model is located far enough. We study in detail the modification of the two single-particle energies by using the equivalent potential in the Schroedinger-like Skyrme-Hartree-Fock equations. The role played by central, kinetic and spin-orbit contributions is discussed. We finally show that the effect of a tensor component in the effective interaction considerably favors the inversion of the two proton states in ^{48}Ca .

PACS numbers: 21.10.Pc, 21.60.-n, 21.60.Jz

I. INTRODUCTION

Novel properties and new scenarios are expected for nuclei situated far from stability. The new generation of radioactive beam facilities will allow to answer many open questions about the peculiarities of these unstable systems. One of the major issues in the physics of exotic nuclei is the study of shell structure and magicity evolution when approaching the drip lines [1, 2]. From a theoretical point of view, two aspects have been underlined as mainly responsible for the evolution of single-particle energies far from stability, the one-body spin-orbit potential which is strongly modified when the surface becomes more diffuse [1] and the tensor force between neutrons and protons in valence sub-shells [3].

Recently, the $N = 28$ shell closure has been experimentally analyzed in the $^{46}\text{Ar}(d, p)^{47}\text{Ar}$ transfer reaction [4]. A strong reduction of the neutron p spin-orbit splitting has been observed in ^{47}Ar with respect to the isotope ^{49}Ca . Since p states are mainly localized in the interior of the nucleus, this strong reduction cannot be justified by the presence of a diffuse surface which would affect only high- l states mainly concentrated at the surface. A theoretical analysis based on the relativistic mean field (RMF) approach has been proposed by Todd-Rutel et al. [5]. It predicts a strong reduction of the spin-orbit splitting for neutron $2p$ -states in ^{46}Ar as compared to ^{48}Ca . At $Z = 20$, the state $2s1/2$ is usually located between $1d5/2$ and $1d3/2$. In the RMF calculations of Ref. [5], however, $2s1/2$ is predicted less bound than $1d3/2$ in both ^{46}Ar and ^{48}Ca ($2s1/2 - 1d3/2$ inversion). In this scenario, $2s1/2$ is empty in ^{46}Ar and occupied in ^{48}Ca : thus, the proton density profile in ^{46}Ar presents a strong depletion in the interior of the nucleus. This reduction of the charge density in the center would be responsible for the modification of the spin-orbit in the nuclear interior and, hence, for the reduction of the neutron $2p$ -splitting.

This problem of $2s1/2 - 1d3/2$ inversion of the proton states has been already analyzed by Campi and Sprung [6] within the Hartree-Fock (HF) + BCS model with an interaction derived from a G-matrix [7]. ^{36}Ar was found as a candidate for this inversion. Skyrme forces do not predict any inversion in this nucleus. It is thus worthwhile to revisit the problem for other nuclei in this region of the nuclear chart in the framework of the Skyrme-HF model.

In this work, we analyze the evolution of the $s - d$ proton single-particle states in Ca isotopes and the possible $2s1/2 - 1d3/2$ inversions. We also present some comparisons with the corresponding results obtained within RMF. We neglect pairing in our treatment since Ca isotopes are proton closed-shell nuclei. We have checked that, within RMF the inclusion of neutron pairing does not modify in a significant way the evolution of the proton states we are interested in. The only important effect due to pairing is the shift of the drip line towards heavier isotopes (for example, the drip line is shifted from ^{60}Ca to ^{76}Ca with the parametrization NL3 [8]). However, this aspect is not relevant in the present analysis which is not intended to make any prediction on the drip line position. We choose the Ca isotopes since experimental signals for the inversion phenomena have been found at least in one of these isotopes, ^{48}Ca : the ground state of ^{47}K (one proton less than ^{48}Ca) is $1/2^+$ with a large spectroscopic factor [9] and the single-particle spectrum of ^{48}Ca has been measured, the proton state $1d3/2$ being more bound than $2s1/2$ by about 300 keV [10]. In our analysis, we explore all the contributions, kinetic, central, spin-orbit and tensor, which can modify the single-particle energies with increasing A and we show that not only the spin-orbit and tensor terms are determinant. The role of the central mean field term is in particular discussed. Within the models which predict the crossing between the two states, we show that this inversion occurs near ^{48}Ca as

well as in very neutron-rich nuclei close to the drip line.

The article is organized as follows. In Sec. II we study the evolution with increasing A of the difference $\Delta\epsilon$ between the $2s_{1/2}$ and $1d_{3/2}$ energies obtained within non-relativistic and relativistic approaches. In Sec. III we concentrate on the non-relativistic case and perform a detailed analysis of the results. The different contributions to $\Delta\epsilon$ are isolated by analyzing them with the equivalent potential in the Schroedinger-like HF equations. In Sec. IV the effect of the tensor force is estimated in the framework of the SLy5-HF [11] model. Finally, conclusions are drawn in Sec. V.

II. EVOLUTION OF $2s_{1/2}$ AND $1d_{3/2}$ PROTON STATES WITHIN SKYRME-HF AND RMF

We first perform a preliminary study with HF calculations of ^{48}Ca using different Skyrme interactions. We then choose three representative forces: SkI5 [12] which predicts a $2s_{1/2} - 1d_{3/2}$ inversion with an energy difference $\Delta\epsilon$ of ~ 800 keV, SGII [13] which also reproduces the inversion ($\Delta\epsilon \sim 200$ keV) and SLy4 [11] for which there is no inversion. With the three selected parametrizations we have systematically analyzed the Ca isotopes from ^{40}Ca up to the HF two-neutron drip line. We recall that, in the three considered Skyrme parametrizations there is no explicit tensor force.

We show in Fig. 1 the difference $\Delta\epsilon$ between the energies of the proton states $2s_{1/2}$ and $1d_{3/2}$ for the three Skyrme forces. The inversion takes place where $\Delta\epsilon$ is positive. Corrections to the individual energies due to the coupling of single particle motion with collective vibrations, which are neglected in our treatment, should be expected (see, for instance, Ref. [14]). However, by considering the energy difference instead of the individual single-particle energies the effects of these corrections should be reduced, the coupling to vibrations having the tendency of shifting upwards the energies of both occupied states.

We observe that the SLy4-HF calculations never predict the $2s_{1/2}$ - $1d_{3/2}$ inversion. On the other hand, both SkI5-HF and SGII-HF predict this inversion around ^{48}Ca as well as for more neutron-rich isotopes starting from ^{58}Ca up to the drip line. The HF two-neutron drip line is located at ^{82}Ca , ^{78}Ca and ^{60}Ca with SkI5, SGII and SLy4, respectively. The two experimental points for ^{40}Ca and ^{48}Ca are also included in the figure. The three sets of results globally present the same behavior. Indeed, in all three cases the quantity $\Delta\epsilon$ starts from a negative value and increases from $A=40$ to $A=48$. This generates a $2s_{1/2}$ - $1d_{3/2}$ inversion with SkI5 (in ^{46}Ca , ^{48}Ca and ^{50}Ca) and with SGII (in ^{48}Ca). Going from ^{48}Ca up to ^{52}Ca the states cross again with SkI5 and SGII, while the distance between them increases with SLy4. Beyond ^{52}Ca $\Delta\epsilon$ increases again with the three parametrizations. This generates another inversion with SkI5 and SGII starting from ^{58}Ca . We notice also that the nuclei for which $\Delta\epsilon$

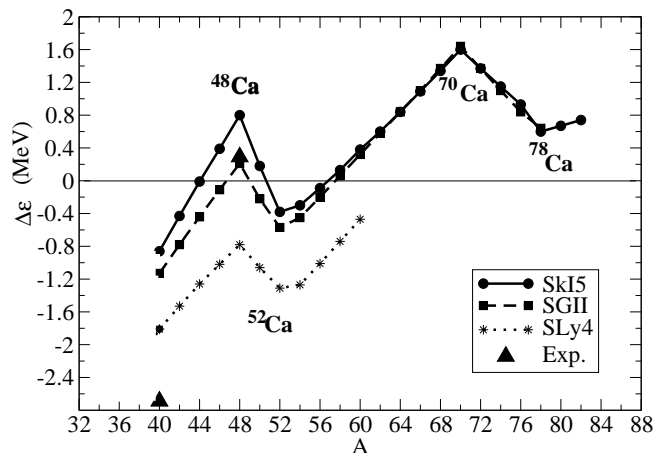


FIG. 1: Difference between the energies of the $2s_{1/2}$ and $1d_{3/2}$ proton states calculated with the Skyrme interactions SkI5, SGII and SLy4 for Ca isotopes.

presents maxima or minima are the same for the three Skyrme forces.

A natural question to ask is whether the above general trends are specific of the Skyrme-HF approach. It is well known that the RMF approach gives a spin-orbit potential whose $(N-Z)$ dependence is somewhat different from that of Skyrme-HF models[15]. We have performed RMF calculations with different parametrizations for the same set of Ca isotopes using the parametrizations DDME1 [16], NL3 [8] and NLB2 [17]. The latter one is chosen as an example of RMF model which does not lead to a $2s_{1/2}$ - $1d_{3/2}$ level inversion. The calculated values of $\Delta\epsilon$ are shown in Fig. 2 up to ^{60}Ca which is the two-neutron drip line isotope predicted by DDME1 and NL3. Globally, we observe for $\Delta\epsilon$ the same trend as that obtained within the non relativistic HF, with maxima and minima corresponding to the same nuclei, ^{48}Ca and ^{52}Ca . Since comparable trends are obtained in both non-relativistic and relativistic approaches we conclude that the calculated evolution of $2s_{1/2}$ and $1d_{3/2}$ states is a generic behavior. We can thus explore more in detail the results by considering only the non-relativistic case.

III. ANALYSIS OF THE CONTRIBUTIONS TO $\Delta\epsilon$

We now concentrate on the maxima and minima of $\Delta\epsilon$. They correspond to nuclei with neutron closed shells or sub-shells: the maximum at ^{48}Ca corresponds to the closure of the neutron $1f_{7/2}$ orbital whereas the minimum at ^{52}Ca corresponds to the filling of the neutron $2p_{3/2}$ state. In the non relativistic Skyrme-HF model the radial HF equations can be expressed in terms of an

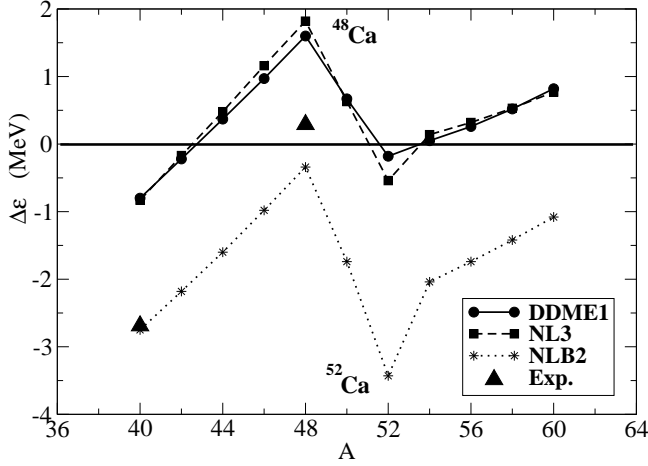


FIG. 2: Difference between the energies of the $2s_{1/2}$ and $1d_{3/2}$ proton states in Ca isotopes calculated in RMF with the parametrizations DDME1, NL3 and NLB2.

energy-dependent equivalent potential V_{eq}^{lj} :

$$\frac{\hbar^2}{2m} \left[-\frac{d^2}{dr^2} \psi(r) + \frac{l(l+1)}{r^2} \psi(r) \right] + V_{eq}^{lj}(r, \epsilon) \psi(r) = \epsilon \psi(r), \quad (1)$$

where

$$V_{eq}^{lj}(r, \epsilon) = V_{eq}^{centr.} + \frac{m^*(r)}{m} U_{so}^{lj}(r) + \left[1 - \frac{m^*(r)}{m} \right] \epsilon, \quad (2)$$

with $U_{so}^{lj}(r) = U_{so}(r) \times [j(j+1) - l(l+1) - 3/4]$. $U_{so}(r)$ is the spin-orbit HF potential and $V_{eq}^{centr.}$ is

$$V_{eq}^{centr.} = \frac{m^*(r)}{m} U_0(r) - \frac{m^{*2}(r)}{2m\hbar^2} \left(\frac{\hbar^2}{2m^*(r)} \right)'^2 + \frac{m^*(r)}{2m} \left(\frac{\hbar^2}{2m^*(r)} \right)'' \quad (3)$$

where $U_0(r)$ is the central HF potentials and $m^*(r)$ is the effective mass [11]. For protons U_0 includes the Coulomb potential. Up to a normalization factor the HF radial wave function ϕ of energy ϵ is related to the solution ψ of Eq.(1) by the relation $\psi = (m^*/m)^{1/2} \phi$. From Eqs. (1)-(3) we can write $\Delta\epsilon$ as

$$\Delta\epsilon = \left[\frac{\langle T \rangle_s}{\langle m^*/m \rangle_s} - \frac{\langle T \rangle_d}{\langle m^*/m \rangle_d} \right] + \left[\frac{\langle V_{eq}^{centr.} \rangle_s}{\langle m^*/m \rangle_s} - \frac{\langle V_{eq}^{centr.} \rangle_d}{\langle m^*/m \rangle_d} \right] - \frac{\langle (m^*/m) U_{so}^{d3/2} \rangle}{\langle m^*/m \rangle_d}, \quad (4)$$

where T is the kinetic contribution. The 3 terms of the r.h.s. of Eq. (4) - kinetic, central and spin-orbit - are plotted in Fig. 3 for the force SkI5 and the nuclei ^{40}Ca ,

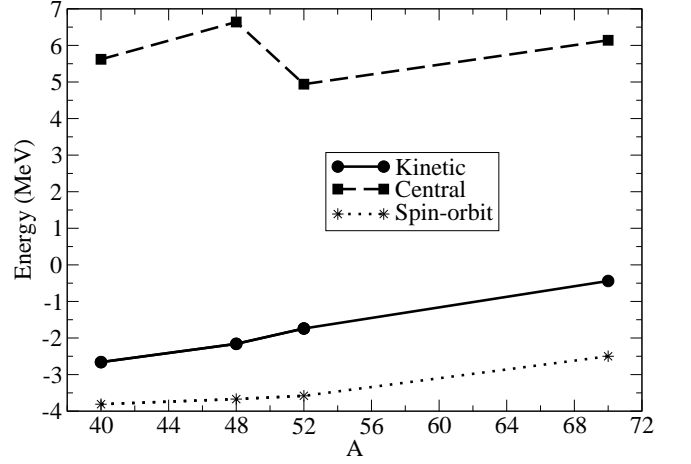


FIG. 3: Kinetic, central and spin-orbit contributions of Eq. (4) for SkI5 in ^{40}Ca , ^{48}Ca , ^{52}Ca and ^{70}Ca .

^{48}Ca , ^{52}Ca and ^{70}Ca . Similar results are obtained with SLy4 and SGII. We mention that the mean value of the effective mass in the denominators of Eq. (4) has very little A-dependence from ^{40}Ca to ^{70}Ca . From Fig. 3, one notices that the spin-orbit and kinetic terms present a regular behavior as a function of A. Both of them are weakened with increasing isospin asymmetry favouring the inversion in very neutron-rich isotopes. The spin-orbit term is weakened because the neutron surface becomes more diffuse with increasing A. In general, the kinetic energy of an orbital depends on the mean distance between its single-particle energy and the bottom of the potential in the region where the wave function is localized. For the two states $2s_{1/2}$ and $1d_{3/2}$ we can look at the difference $\epsilon_{lj} - V_{eq}^{lj}(r_0)$, where r_0 is the root mean square (r.m.s.) radius of the corresponding wave function. The evolution of V_{eq}^{lj} with increasing A is governed by two effects: i) the lowering of the proton potential due to the symmetry term; ii) the formation of a neutron skin which modifies the proton distribution by pulling it towards larger radii. The intensity of these two effects depends on the quantum numbers of the neutron orbitals which are filled and of the proton wave function under study. As an illustration, we consider ^{52}Ca and ^{70}Ca . The r.m.s. radii r_0 and the values $\epsilon_{lj} - V_{eq}^{lj}(r_0)$ are shown in Table I for the $2s_{1/2}$ and $1d_{3/2}$ states. From ^{52}Ca to ^{70}Ca the difference $\epsilon_{lj} - V_{eq}^{lj}(r_0)$ is reduced more for $1d_{3/2}$ (4.9%) than for $2s_{1/2}$ (0.4%). This analysis is confirmed by the evolution of the two r.m.s. radii. It is evident that, going from ^{52}Ca to ^{70}Ca , the $1d_{3/2}$ wave function is more affected than $2s_{1/2}$ by the enlarging of the potential due to the formation of a thick neutron skin. This explains the increase of the kinetic contribution to $\Delta\epsilon$ with the neutron number. We consider now the central term of Eq.(4) which is responsible for the maxima and minima of $\Delta\epsilon$, and concentrate on the maximum at ^{48}Ca . We mention that the major role played by the

A	r_0 (fm)	r_0 (fm)	$\epsilon - V_{eq}^{lj}(r_0)$ (MeV)	$\epsilon - V_{eq}^{lj}(r_0)$ (MeV)
	2s1/2	1d3/2	2s1/2	1d3/2
52	3.71	3.70	23.11	19.73
70	3.81	3.89	23.01	18.76

TABLE I: The values of r_0 and $\epsilon - V_{eq}^{lj}(r_0)$, for the states 2s1/2 and 1d3/2 in ^{52}Ca and ^{70}Ca . The interaction is SkI5.

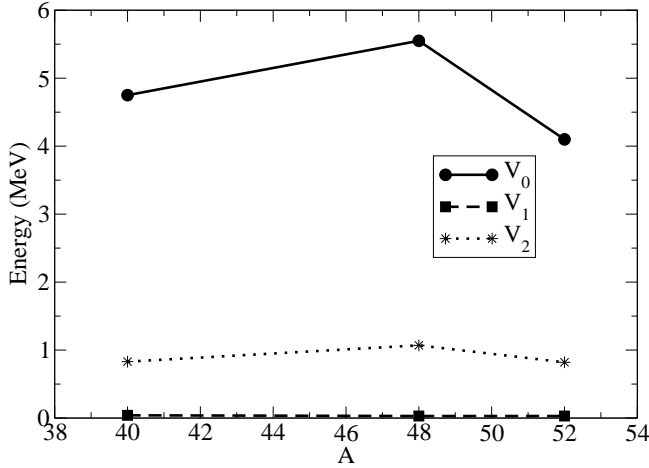


FIG. 4: V_0 , V_1 and V_2 calculated with SkI5 in ^{40}Ca , ^{48}Ca and ^{52}Ca .

central term in modifying the single particle energies has been also underlined by Gaudetroy et al. [4]. We introduce the quantities V_0 , V_1 and V_2 which correspond to the contributions of the 3 terms of Eq. (3). They are plotted in Fig. 4 for ^{40}Ca , ^{48}Ca and ^{52}Ca . It turns out that the term mainly affected by the neutron shell structure is V_0 which contains the Hartree-Fock potential.

We can separate the energy contributions of the $N=Z=20$ core from those of the excess neutrons. For instance, the total nucleon density ρ is a sum of ρ_{core} and ρ_{excess} , and similarly for the other types of densities. Then, for any HF quantity the core contribution is obtained by replacing in its expression the total densities by core densities whereas the neutron excess contribution corresponds to the rest. We show in Fig. 5 the core and neutron excess contributions to V_0 . It is clear that the change of slope at ^{48}Ca is mainly due to the neutron excess contribution. We have further verified that the term mainly responsible is the t_0 term of the Skyrme force. The density-dependent term (t_3 term) is also sensitive to the neutron shell structure but with an opposite behavior reducing the effect due to the t_0 term. Hence, the main parameters which influence the behavior of $\Delta\epsilon$ are x_0 and t_0 as well as x_3 , t_3 and α . We have checked that the role played by the other terms of the HF potential is negligible.

To complete our analysis we consider separately the two single-particle energies 2s1/2 and 1d3/2. We have

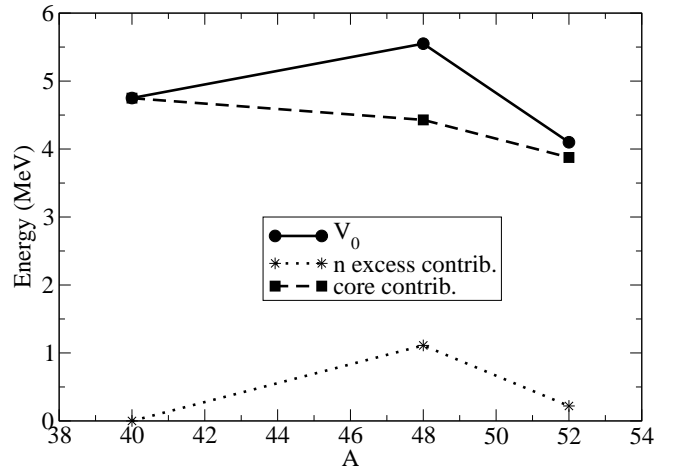


FIG. 5: Core and neutron excess contributions to V_0 for SkI5 in ^{40}Ca , ^{48}Ca and ^{52}Ca .

verified that the maximum of $\Delta\epsilon$ at ^{48}Ca is mostly due to the energy of the 1d3/2 state which decreases less rapidly from ^{48}Ca to ^{52}Ca than from ^{40}Ca to ^{48}Ca . This behavior is explained in Fig. 6. In the top panels the neutron excess contribution P_{HF} to the HF potential due to the t_0 and t_3 terms is plotted for ^{44}Ca , ^{48}Ca and ^{52}Ca (see e.g. [11] for the expressions in terms of the Skyrme force parameters). In the middle panels we show the squares of the 1d3/2 and 2s1/2 radial wave functions multiplied by r^2 . In the bottom panels the products $P_{HF}|\phi|^2r^2$ are shown. Since P_{HF} is negative (the t_0 contribution is negative and the largest in absolute value) the proton single-particle energies are lowered with increasing N-Z, as expected. We observe that, in ^{44}Ca and ^{48}Ca the potential related to the neutron excess (1f7/2 neutron orbital) is concentrated in the region where the 1d3/2 wave function is localized. The overlap with this wave function is thus the largest and this explains why the filling of the neutron 1f7/2 orbital has an important effect on the proton 1d3/2 energy which is strongly lowered. On the other hand, when the neutron 2p3/2 orbital is filled (from ^{48}Ca to ^{52}Ca) the potential changes very little in the region where the 1d3/2 wave function is appreciable. This explains why the 1d3/2 energy decreases more from A=44 to 48 than from A=48 to 52. The energy of the 2s1/2 proton state is much less sensitive to the neutron shell structure in these isotopes and it decreases rather monotonically from A=44 to 52.

IV. TENSOR FORCE EFFECT

The tensor force plays certainly a role in the evolution of single-particle states. This is discussed, e.g., in the framework of the shell model in ref. [3]. In a mean field approach, the tensor effect originates from the π -nucleon and ρ -nucleon contributions to the Fock terms

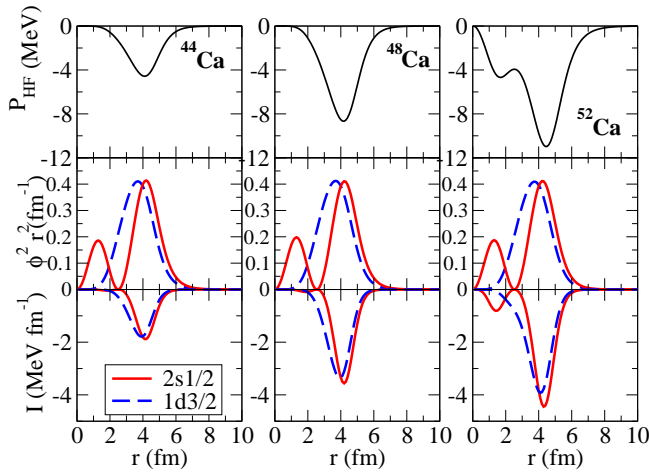


FIG. 6: Potential P_{HF} (see text) (top), square of $1d3/2$ and $2s1/2$ radial wave functions times r^2 (middle) and their product (bottom) calculated with SkI5 in ^{44}Ca , ^{48}Ca and ^{52}Ca .

[18, 19], and it can be introduced phenomenologically in the parametrizations of effective interactions built for HF models [20, 21, 22]. Recent progress have been made in determining the tensor terms of Skyrme interactions [23, 24] by adjusting the single-particle spectra measured in $N=82$ isotones and $Z=50$ isotopes [25].

When this force is included the spin-orbit potential presents an additional term depending on the spin density J , namely,

$$U_{so}^q = \frac{W_0}{2}(\nabla\rho + \nabla\rho_q) + \alpha J_q + \beta J_{q'} , \quad (5)$$

where q stands for neutrons (protons) and q' for protons (neutrons), α and β consist of a sum of central and tensor contributions: $\alpha = \alpha_C + \alpha_T$, $\beta = \beta_C + \beta_T$. The central contributions depend only on the velocity-dependent part of the Skyrme force whereas the tensor contributions are generated by the tensor component of the Skyrme force [21, 24].

To estimate the effect of the tensor force in our case we use the Skyrme force SLy5 which already contains in the fitting protocol the terms α_C and β_C . For α_T and β_T we adopt the values determined in Ref. [23] by comparing the Skyrme-HF predictions with the data of Ref. [25]. These values are $\alpha_T = -170 \text{ MeV fm}^5$ and $\beta_T = 100 \text{ MeV fm}^5$. We expect that the tensor force favors the inversion in ^{48}Ca (see for instance Fig. 4 of Ref. [3]). Actually, from ^{40}Ca to ^{48}Ca the $1f7/2$ neutron orbital is filled. The interaction between the proton orbital $1d3/2$ and the neutron orbital $1f7/2$ is attractive and its effect is to lower the energy of $1d3/2$, thus favoring the crossing with $2s1/2$. As an illustration we performed SLy5-HF calculations for ^{40}Ca , ^{48}Ca , ^{52}Ca and ^{70}Ca (^{70}Ca is still bound within SLy5-HF). We show in Fig 7 the values of $\Delta\epsilon$ obtained with and without the tensor contribution. As expected, the tensor force increases the slope

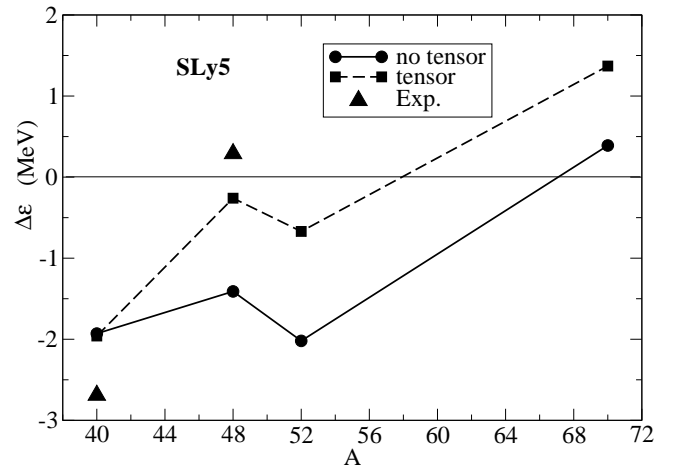


FIG. 7: Difference between the energies of $2s1/2$ and $1d3/2$ proton states in ^{40}Ca , ^{48}Ca , ^{52}Ca and ^{70}Ca calculated with SLy5 with and without the tensor contribution.

going from ^{40}Ca to ^{48}Ca bringing the two states close together and improving the agreement with the experimental data. The improvement is quite strong since the value of $\Delta\epsilon$ in ^{48}Ca is equal to -0.26 MeV and -1.41 MeV with and without the tensor contribution, respectively.

V. SUMMARY

In this article we have analyzed the modification of the proton single-particle states $2s1/2$ and $1d3/2$ in Ca isotopes within the non-relativistic Skyrme-HF and the relativistic RMF models. Pairing effects have been neglected since Ca isotopes are proton closed-shell. We are interested in the evolution of proton states and the inclusion of neutron pairing does not affect significantly the global trend of our results. Both models, HF and RMF, predict the same evolution with increasing A for the difference $\Delta\epsilon$ of the energies of the two states. This evolution depends on the neutron orbitals which are filled, $\Delta\epsilon$ presenting maxima and minima corresponding to neutron shell or sub-shell closures. In particular, going from ^{40}Ca to ^{48}Ca the two proton states come closer to each other and they can sometimes cross in some models. By performing an analysis based on the equivalent potential in the non-relativistic Skyrme-HF approach, we have shown that the kinetic and spin-orbit contributions present quite a regular behavior with increasing A . They both strongly favor the inversion of the two states in very neutron-rich nuclei. We have also verified that the contribution which is mostly responsible for the maximum of $\Delta\epsilon$ at ^{48}Ca (and leading to an inversion for some models) is the central HF potential and, in particular the t_0 and t_3 terms. The former term favors the crossing of the two states near ^{48}Ca whereas the latter acts against it. The net effect is that the two states get closer and can cross each other in

some models.

We have finally analyzed the role of the tensor force within the SLy5-HF model and found that its contribution goes in the same direction as the t_0 term of the HF potential, favoring the inversion of the states near ^{48}Ca .

Our analysis was restricted to a purely mean field picture. Work should be done to include effects beyond mean field. For instance, particle-phonon coupling, which has been neglected here, is expected to improve the quality of the theoretical predictions in the study of

single-particle states evolution.

The authors thank K. Bennaceur, A. Bhagwat, G. Colò, L. Gaudefroy, H. Sagawa and O. Sorlin for valuable discussions. ZYM and NVG acknowledge the partial support of CNRS-IN2P3 (France) under the PICS program, of the National Natural Science Foundation of China under Nos.10475116, 10535010 and the European Community project Asia-Europe Link in Nuclear Physics and Astrophysics CN/Asia-Link 008(94791).

-
- [1] J. Dobaczewski, I. Hamamoto, W. Nazarewicz, and J.A. Sheich, Phys. Rev. Lett. **72**, 981 (1994)
 - [2] E. Becheva, et al., Phys. Rev. Lett. **96**, 012501 (2006).
 - [3] T. Otsuka, T. Suzuki, R. Fujimoto, H. Grawe, and Y. Akaishi, Phys. Rev. Lett. **95**, 232502 (2005).
 - [4] L. Gaudefroy, et al., Phys. Rev. Lett. **97**, 092501 (2006).
 - [5] B.G. Todd-Rutel, J. Piekarowicz, and P.D. Cottle, Phys. Rev. **C 69**, 021301(R) (2004).
 - [6] X. Campi and D.W.L. Sprung, Phys. Lett. **46 B**, 291 (1973).
 - [7] D.W.L. Sprung and P.K. Banerjee, Nucl. Phys. **A 168**, 273 (1971).
 - [8] G.A. Lalazissis, J. Koenig, and P. Ring, Phys. Rev. **C 55**, 540 (1997).
 - [9] C.A. Ogilvie, et al., Nucl. Phys. **A 465**, 445 (1987).
 - [10] Database of the National Nuclear Data Center, Brookhaven; T.W. Burrows, Nuclear Data Sheets Update for A=47. Nucl. Data Sheets **74**, 1 (1995); J.S. Hanspal, et al., Nucl. Phys. **A 436**, 236 (1985); S. Fortier, et al., Nucl. Phys. **A 311**, 324 (1978).
 - [11] E. Chabanat, et al., Nucl. Phys. **A 627**, 710 (1997); *ibid.* **A 635**, 231 (1998); *ibid.* **A 643**, 441 (1998).
 - [12] P.-G. Reinhard, H. Flocard, Nucl. Phys. **A 584**, 467 (1995).
 - [13] N.V. Giai and H. Sagawa, Phys. Lett. **B 106**, 379 (1981);
 - N.V. Giai and H. Sagawa, Nucl. Phys. **A 371**, 1 (1981).
 - [14] P. Donati, et al., Phys. Rev. Lett. **84**, 4317 (2000).
 - [15] G.A. Lalazissis, D. Vretenar, W. Pöschl, and P. Ring, Phys. Lett. **B 418**, 7 (1998); G.A. Lalazissis, D. Vretenar, and P. Ring, Phys. Rev. **C 57**, 2294 (1998).
 - [16] T. Niksic, D. Vretenar, P. Finelli, and P. Ring, Phys. Rev. **C 66**, 024306 (2002).
 - [17] A. Boussy, S. Marcos, and J.-F. Mathiot, Nucl. Phys. **A 415**, 497 (1984); A. Boussy, S. Marcos, and Pham van Thieu, Nucl. Phys. **A 422**, 541 (1984).
 - [18] W.H. Long, N. Van Giai, and J. Meng, Phys. Lett. **B 640**, 150 (2006).
 - [19] W.H. Long, H. Sagawa, J. Meng, and N. Van Giai, arXiv:nucl-th/0609076
 - [20] T.H.R. Skyrme, Nucl. Phys. **9**, 615 (1959).
 - [21] Fl. Stancu, D.M. Brink, and H. Flocard, Phys. Lett. **B 68**, 108 (1977).
 - [22] T. Otsuka, T. Matsuo, and D. Abe, Phys. Rev. Lett. **97**, 162501 (2006).
 - [23] G. Colò, H. Sagawa, S. Fracasso, and P.F. Bortignon, Phys. Lett. **B 646**, 227 (2007).
 - [24] D.M. Brink and Fl. Stancu, arXiv:nucl-th/0702065
 - [25] J.P. Schiffer, et al., Phys. Rev. Lett. **92**, 162501 (2004).